COLORED STONES AND ORGANIC MATERIALS

Visit to andesine mines in Tibet and Inner Mongolia. Gem-quality plagioclase feldspar (labradorite) has been recovered for years from the U.S. state of Oregon (e.g., A. M. Hofmeister and G. R. Rossman, "Exsolution of metallic copper from Lake County labradorite," *Geology*, Vol. 13, 1985, pp. 644–647; C. L. Johnston et al., "Sunstone labradorite from the Ponderosa mine, Oregon," Winter 1991 *Gems & Gemology*, pp. 220–233). In 2002, red andesine-labradorite appeared in the gem market that was reportedly sourced from an unspecified locality in the Democratic Republic of the Congo (Spring 2002 GNI, pp. 94–95), but some believe that this material actually came from China. In late 2005, a red andesine called "Tibetan sunstone" was supplied by Do Win Development Co. Ltd. of Tianjin, China, reportedly from Nyima (actually Nyemo) in central Tibet (Winter 2005 GNI, pp. 356–357). Then, at the February 2007 Tucson gem shows, King Star Jewellery Co. (Hong Kong) and M. P. Gem Corp. (Kofu, Japan) introduced a similar red andesine from Tibet called "Lazasine." A large supply of red andesine allegedly from China was offered for sale as an official gemstone of the 2008 Summer Olympic Games in Beijing. Despite claims to the contrary, there has been widespread suspicion that the red Chinese andesines are diffusion treated. In fact, recent studies have proved the viability of diffusion-treating such material (e.g., G. Roskin, "JCK web exclusive: The andesine report," posted November 12, 2008, www.jckonline.com/article/CA6613857.html).

In October-November 2008, this contributor visited two andesine deposits in the Chinese autonomous regions of Tibet and Inner Mongolia. The investigation was made possible by the cooperation of mine owners Li Tong of Tibet and Wang Gou Ping of Inner Mongolia, as well as trip organizers Wong Ming (King Star Jewellery Co.) and Christina Iu (M. P. Gem Corp.), who are partners in the Tibetan andesine mine. Also participating in the expedition were Masaki Furuya (Japan Germany Gemmological Laboratory, Kofu, Japan), David Chiang (BBJ Bangkok Ltd., Bangkok), and Marco Cheung (Litto Gems Co. Ltd., Hong Kong).

The Tibetan andesine mine we visited is located 70 km south of the region's second largest city, Xigazê (or Shigatse), in southern Tibet. This area is well south of the Nyima/Nyemo area (Lhasa region), and our guides were not aware of an andesine mine in that part of Tibet. We drove seven hours from the capital city of Lhasa to the mine, which lies at an elevation of more than 4,000 m. The site is divided into north and south areas with a total coverage spanning 3–4 km east-west and 5–7 km north-south. During our visit, fewer than 10 miners were digging pits in the south area, near a piedmont riverbed (located at the base of a mountain). Organized mining began there in January 2006 under the supervision of Li Tong. The work is done by hand, from April to November. According to the miners, red andesine was originally found in this area in the 1970s, and beads of this material first appeared in Lhasa's largest bazaar (Bakuo Street) in 2003.

The surface layer at the site consists of humic soil that is 0.5–3 m thick. The andesine is mined from an underlying layer consisting of greenish gray or dark gray sand/gravel in the south area (figures 1 and 2), and yellowish red or greenish gray soil in the north area. The andesine-bearing layers are apparently derived from Tertiary volcano-sedimentary

Editor's note: Interested contributors should send information and illustrations to Brendan Laurs at blaurs@gia.edu or GIA, The Robert Mouawad Campus, 5345 Armada Drive, Carlsbad, CA 92008. Original photos can be returned after consideration or publication.

GEMS & GEMOLOGY, Vol. 44, No. 4, pp. 369–379

Figure 1. The andesine-bearing deposits in Tibet are exploited in a series of tunnels, with the miners using simple hand tools. Photo by A. Abduriyim.

Figure 2. Rounded crystals of Tibetan andesine are found in concentrations mixed with sand/gravel or soil. Photo by A. Abduriyim.

deposits (Qin Zang Gao Yuan [Tibet Highland] area geologic map, Chengdu Institute of Multipurpose Utilization of Mineral Resources, China Geological Survey, Chengdu, Sichuan Province, 2005). In the south mining area, a few tunnels penetrate several meters horizontally into the andesine-bearing horizons. In addition, a shaft was sunk several meters deep in the north area, but mining there was discontinued after the devastating Chengdu earthquake in May 2008. The andesine is concentrated in patches consisting of several to more than a dozen pieces (100–200 g total) mixed with sand/gravel or soil (again, see figure 2). These accumulations appear to have been concentrated across a wide area by water from seasonal snowmelt.

Alluvial transport has rounded the crystals, and most were found as translucent to transparent pebbles that were <1 cm in diameter (figure 3), though the largest pieces reached 4 cm. Most were orangy red; deep red material was less common. Some had areas that were green or colorless, but we did not see any pieces that were completely brown, yellow, or colorless. The annual production from the region is estimated to be 700–800 kg, of which 30–50 kg are gem

Figure 3. The Tibetan andesine consists mainly of orangy red pebbles that are <1 cm in diameter. Photo by A. Abduriyim.

Figure 4. This horizon has produced andesine in the Guyang area of Inner Mongolia. Photo by Wong Ming.

Figure 5. These andesine pebbles (2–5 cm) were mined from the Inner Mongolian village of Shuiquan. Photo by A. Abduriyim.

quality. A visit to mountain peaks in the mining area revealed Jurassic volcanic rocks and detrital deposits; a volcanic origin is also the case for similar feldspar from Oregon.

The andesine from Inner Mongolia is mined from an alluvial deposit of sand/gravel in the Guyang area, north of Baotou city. The mine is situated in the Yinshan tectonic belt of Mesozoic-Cenozoic age (Inner Mongolia Guyang-Xiaoyutai area geologic map, Inner Mongolia Autonomous Region Geological Survey, Hohhot, 1982). Andesine has been recovered from a region measuring 20 km east-west and 5 km north-south. Humic topsoil overlies Tertiary (Pliocene) and Cretaceous sand/gravel; some areas also show layers of tuff or basaltic rock. The andesine is restricted to a light gray layer (locally iron stained) that is 1–3 m thick and lies several meters beneath the surface—down to more than 10 m—within the sand/gravel (figure 4). Organized mining has taken place near Shuiquan and Haibouzi villages, producing up to 100 tonnes annually. The andesine seen by this contributor commonly had high transparency and was somewhat rounded, except for broken pieces that showed well-developed cleavage surfaces. The stones were typically 0.3–5.5 cm in diameter, with 70–80% in the 1–2 cm range (figure 5). Most of the andesine was pale yellow. Colorless or deep yellow stones were uncommon, while other colors have not been reported from this area.

This field investigation confirmed that the Xigazê region of Tibet does indeed produce natural red andesine, while the Guyang area of Inner Mongolia is a source of pale yellow andesine that may be used as the starting material for diffusion treatment. Additional images from this expedition can be found in the *G&G* Data Depository at www.gia.edu/gemsandgemology.

Ahmadjan Abduriyim
(ahmadjan@gaaj-zenhokyo.co.jp)
Gemmological Association of All Japan – Zenhokyo
Tokyo, Japan

Gemological properties of andesine collected in Tibet and Inner Mongolia. While visiting andesine mines in Tibet and Inner Mongolia (see previous GNI entry), one of these contributors (AA) obtained several samples for gemological study that he witnessed being gathered by the miners. Ten pieces (up to 26.0 g; see, e.g., figure 6) from each region were polished with two parallel windows, and all were characterized for this report. It is currently impossible to unequivocally determine in the laboratory whether red andesine in the gem trade has been diffusion treated. This preliminary characterization was done to gather data on red samples that are known to be untreated, as well as pale yellow material that may be used as a starting material for diffusion treatment.

Figure 6. These are some of the samples of andesine obtained in Tibet (top, up to 5.4 g) and Inner Mongolia (bottom, up to 26.0 g, some partially polished) that were examined for this report. Photos by M. Kobayashi.

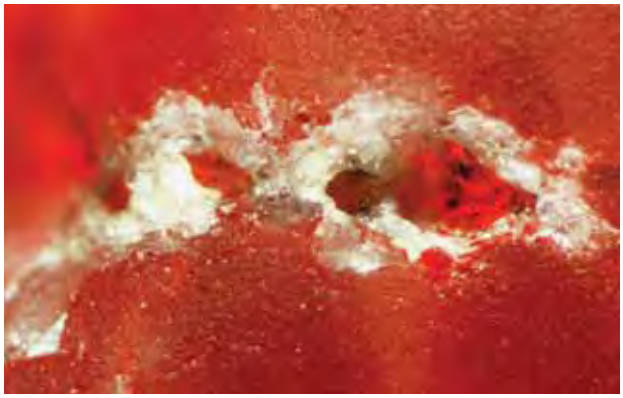

Figure 7. Surface etching was observed on some Tibetan andesine pebbles. Photomicrograph by A. Abduriyim; magnified 28×.

All the samples had a waterworn appearance, and some of the Tibetan pebbles also had embayed areas that appeared to have been created by chemical etching (figure 7). The pebbles from Inner Mongolia also were abraded, but they were more angular than the Tibetan samples and exhibited conchoidal fractures.

The Tibetan samples had the following gemological properties: color—brownish red to orange-red to red; pleochroism—weak; RI—1.550–1.561; birefringence—0.009; optic sign—biaxial positive; SG—2.69–2.72; fluorescence—orange to long-wave, and dark red to short-wave, UV radiation; and Chelsea filter reaction—red. The Inner Mongolian samples were pale yellow, but otherwise they exhibited almost identical properties except that they were inert to both long- and short-wave UV radiation, and they showed no reaction to the color filter.

Examination with a gemological microscope revealed that most of the Tibetan samples contained prominent twin lamellae and parallel lath-like hollow channels (figure 8, left), irregular dislocations (figure 8, right), and irregular color patches caused by milky turbidity from fine granular inclusions (figure 9). One of the polished samples displayed aventurescence due to the presence of native-copper platelets. The samples from Inner Mongolia contained parallel flat growth tubes (figure 10, left), as well as abundant linear fissures (figure 10, right) and fine twin planes arranged parallel to a (010) direction. In some cases, the linear fissures caused a weak opalescence, and such stones cut *en cabochon* would be expected to show a weak cat's-eye effect. Cleavage planes were also well developed along one (010) direction.

Absorption spectra were measured with a UV-Vis spectrometer in the range 220–860 nm. The Tibetan andesine exhibited absorption from 320 nm toward shorter wavelengths, as well as a prominent broad band near 565 nm due to colloidal copper. In addition, a weak feature near 380 nm was due to Fe^{3+}. Similar absorptions have been documented in red andesine that was reportedly from the Democratic Republic of the Congo and in red labradorite from Oregon (A. M. Hofmeister and G. R. Rossman, "Exsolution of metallic copper from Lake County labradorite," *Geology*, Vol. 13, 1985, pp. 644–647; M. S. Krzemnicki, "Red and green labradorite feldspar from Congo," *Journal of Gemmology*, Vol. 29, No. 1, 2003, pp. 15–23). Spectroscopy in the near-infrared region (800–2500 nm) revealed an absorption peak near 1260 nm that is caused by Fe^{2+}.

The andesine from Inner Mongolia showed absorptions at 380, 420, and 450 nm. The 380 nm feature was strongest, while the broad band at 420 nm (presumably due to charge transfer between Fe^{2+} and Fe^{3+}) was characteristic. A strong and broad absorption also was observed near 1260 nm.

Energy-dispersive X-ray fluorescence (EDXRF) chemical analysis of andesine from both Tibet and Inner Mongolia revealed very similar compositions, with 55–56 wt.% SiO_2, 26–27 wt.% Al_2O_3, 10 wt.% CaO, and 5.8–6.2 wt.% Na_2O. Trace elements such as K, Mg, Ti, Fe, and Sr were detected. The Tibetan stones also contained 0.06–0.10 wt.% CuO, but no Cu was detected in the Inner Mongolian samples. The chemical composition showed that all samples were andesine, with some plotting at the border with labradorite ($An_{47–50}$). Previous electron microprobe analyses of samples from Inner Mongolia showed they were labradorite, with a composition of $An_{50–51}$ (or $An_{52–53}$ if K is excluded; Y. Cao, "Study on the feldspar from Guyang County, Inner Mongolia and their color enhancement," Master's thesis, Geological University of China, 2006).

Laser ablation–inductively coupled plasma–mass spectrometry (LA-ICP-MS) analysis showed that samples from

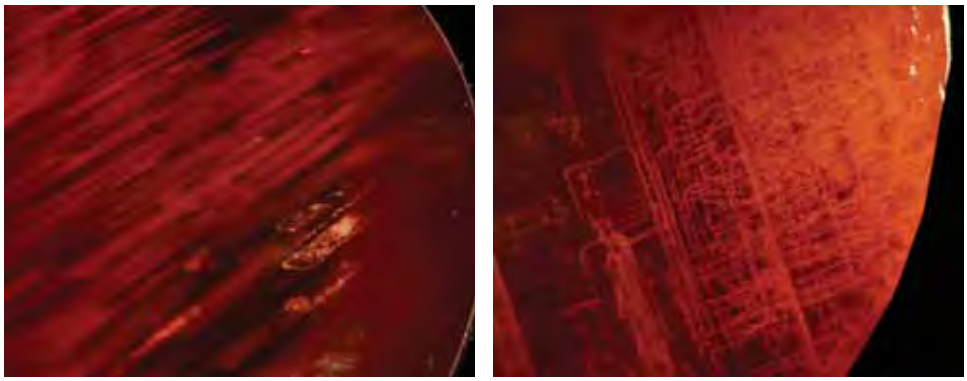

Figure 8. With magnification, twin lamellae and parallel lath-like hollow channels are seen in this orangy red andesine from Tibet (left, magnified 25×). Also present were distinctive dislocation features (right, magnified 20×). Photomicrographs by A. Abduriyim.

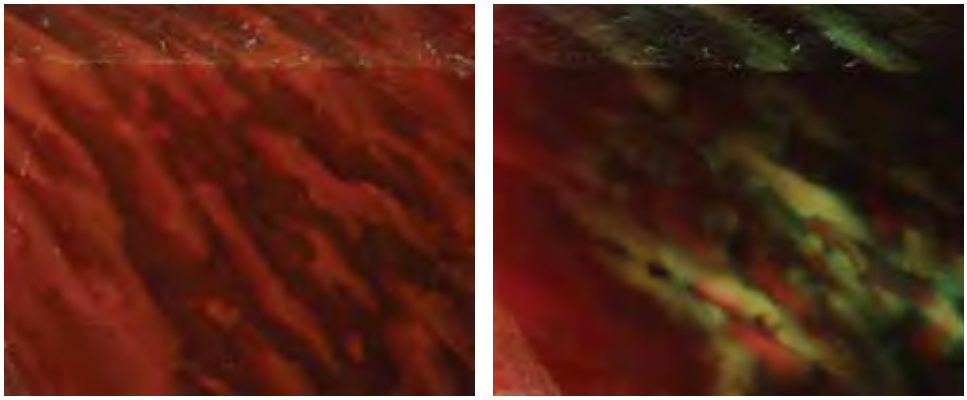

Figure 9. This Tibetan andesine exhibits concentrated areas of red and orange-red milky turbidity (left). When viewed with diffused light, some of these areas appear green or near colorless (right). Photomicrographs by A. Abduriyim; magnified 25×.

both localities contained several trace elements: K (2200–3600 ppm), Fe (1000–3200 ppm), Sr (700–1000 ppm), Mg (330–620 ppm), Ti (400–510 ppm), Ba (120–160 ppm), Mn (20–40 ppm), Ga (20–30 ppm), Li (10–60 ppm), and Sc (5–15 ppm); B, V, Co, Zn, Rb, Sn, Ce, and Eu were <3 ppm each. No significant elemental difference was observed between Tibetan and Mongolian andesine, other than Cu content: 300–600 ppm in orangy red andesine, and <3 ppm in pale yellow andesine. In addition, Li was slightly dominant in Tibetan andesine.

Additional images from this study can be found in the *G&G* Data Depository at www.gia.edu/gemsandgemology.

Ahmadjan Abduriyim and Taisuke Kobayashi
Gemmological Association of All Japan – Zenhokyo
Tokyo, Japan

New find of vivid kunzite from Pala, California. In July 2008, several etched crystals of gem-quality kunzite were found at the historic Elizabeth R mine, located on Chief Mountain in the Pala District of San Diego County (see, e.g., Fall 2001 GNI, pp. 228–231). In mid-2008, Jeff Swanger (Escondido, California) purchased the mine from Roland Reed (El Cajon, California). Mr. Reed has continued to work the Elizabeth R while Mr. Swanger mines the neighboring Ocean View property, where he found a large gem pocket in 2007 (see Spring 2008 GNI, pp. 82–83).

Although this was not the first kunzite discovery at the Elizabeth R, these pieces had a particularly vibrant pinkish purple to pink-purple color that is seldom seen in natural-color kunzite (e.g., figures 11 and 12). Mr. Reed believes they compare favorably to kunzite from the nearby Vandenberg mine, which produced colors that are considered among the finest found anywhere. Approximately 0.5 kg of top-grade material has been recovered, and the best pieces were sent for fashioning to Minas Gem Cutters of Los Angeles. So far 11 stones have been cut, and the two largest ones weighed 57 and 28 ct. The cut material is being sold through Pala International (Fallbrook, California).

The samples shown in figure 12 were examined microscopically by this contributor. The few internal features were typical for kunzite: elongated, tapered etch tubes; and two-phase (liquid and gas) inclusions—either alone, in parallel, or in a "fingerprint" pattern with irregular to rounded elongate shapes. No mineral inclusions were seen. One faceted stone contained very slight cleavage feathers on the pavilion, while the rough piece showed typical shield-shaped etch marks on its surface.

Kunzite is challenging to cut because of its cleavage, twin planes, and sensitivity to vibrations and thermal shock. It also has a reputation as an "evening" gem, since its color fades with prolonged exposure to light or heat. Kunzite can naturally show an attractive color, as in this new find from the Elizabeth R mine, or the purple-pink hue can be produced by irradiating (and annealing) pale or colorless spodumene. Most natural-color kunzite is light pink. This new production from Pala serves as a reminder that gem mining is still active in San Diego County, where kunzite was initially discovered more than 100 years ago.

Michael Evans (mevans@gia.edu)
GIA, Carlsbad

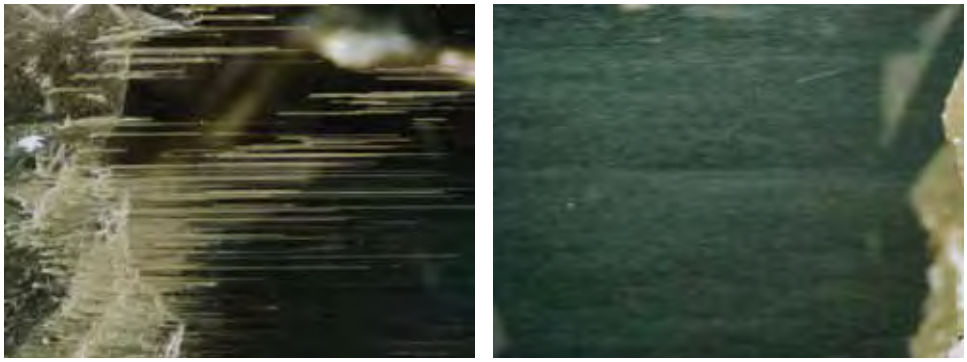

Figure 10. Dense concentrations of parallel growth tubes were common in the pale yellow andesine from Inner Mongolia (left). In some samples, linear fissures (right) caused weak opalescence. Photomicrographs by A. Abduriyim; magnified 20×.

Figure 11. These kunzite crystals (up to ~4.3 cm long) were recovered in July 2008 from the Elizabeth R mine in San Diego County. Photo by Mark Mauthner.

Figure 12. A number of fine faceted samples have been polished from the new Elizabeth R kunzite find. The crystal weighs 11.5 g and the cut stones are 12.47–19.32 ct. Photo by Robert Weldon.

Natural pearls of the Veneridae family. The best-known natural pearls from bivalves of the Veneridae (classified by Rafinesque, 1815) family are those from *Mercenaria mercenaria* (Linnaeus, 1758), also known as "quahog" pearls from the mollusk's common name, northern quahog. These non-nacreous pearls range from "cream" white to brown, and from faint pinkish purple to dark purple, though some are pure white (e.g., figure 13). Like other natural pearls, quahog pearls are seldom perfectly round; in rare cases, circled quahog pearls occur (figure 14). *M. mercenaria* bivalves are found along the Atlantic coast of North America to the Yucatan Peninsula. The species also has been introduced along California's Pacific coast.

However, *M. mercenaria* is not the only mollusk of the *Mercenaria* genus to produce pearls. White, "cream," and sometimes brown non-nacreous pearls can be found in another species belonging to the same genus, *M. campechiensis* (Gmelin, 1791), or southern quahog. This species is found in the southern part of the *M. mercenaria* distribution area. *M. campechiensis* is slightly larger than *M. mercenaria*, and its interior surface lacks purple coloration; thus, it cannot produce purple pearls.

Nor are *Mercenaria* bivalves the only mollusks of the Veneridae family that can produce beautiful pearls. In the Fall 2001 GNI section (p. 233), one of these contributors (EF) described an almost perfectly round purple pearl found along the coast of France in a mollusk from the *Venerupis* genus (Lamarck, 1818), *V. affinis decussata* (Linnaeus, 1758). This mollusk (known as "palourde" in French) is commonly harvested for its meat, which is considered a delicacy.

The interiors of *M. mercenaria* and *V. aff. decussata* shells, as well as the pearls associated with them, are similar in appearance (figure 15). The purple color is present at the shell margins, mainly around the muscle scars. Both pearls and shells display the same medium chalky whitish yellow fluorescence to long- and short-wave UV radiation, though it is weaker for the *V. aff. decussata*.

Raman spectroscopy of the samples in figure 13 (left

Figure 13. These two photos illustrate natural "quahog" pearls from the M. mercenaria *mollusk. The white button-shaped sample (left image, far left) is ~10.5 × 7.8 mm (8.17 ct), and the brown button-shaped pearl in the right image is ~9.3 × 7.5 mm (5.03 ct). Courtesy of P. Lançon, Geneva; photos by Thomas Notari.*

*Figure 14. Note in these four baroque quahog (*M. mercenaria*) pearls that color variation in the bicolored samples is distributed along the pearls' rotational axis. All are circled except the second sample from the left, but its ovoid shape is still probably due to pearl rotation during formation. The bicolored sample on the left is ~13.2 × 11.2 mm (11.62 ct). Courtesy of P. Lançon, Geneva; photo by Thomas Notari.*

image) and figure 14, using 488, 514, and 561 nm laser excitations, showed that the purple color was due to a mixture of unsubstituted polyenic (polyacetylenic) compounds (figure 16). To our knowledge, the origin of the purple color of Veneridae pearls and/or inner shells has not been previously reported. Similar pigments have been

*Figure 16. These Raman spectra for a purple quahog (*M. mercenaria*) pearl were taken at laser excitations of 488, 514, and 561 nm. In the region most "sensitive" to C=C stretching bonds (about 1500 cm^{-1}, see inset), variations in the position, shape, and relative intensities of the peaks are quite apparent. This suggests that the purple color is due to a mixture of unsubstituted polyenic (polyacetylenic) compounds and not to a single pigment. Raman spectra on colored samples from* V. aff. decussata *showed the same peaks. All the peaks are normalized to the main aragonite peak at 1086 cm^{-1}. The spectra are offset vertically for clarity.*

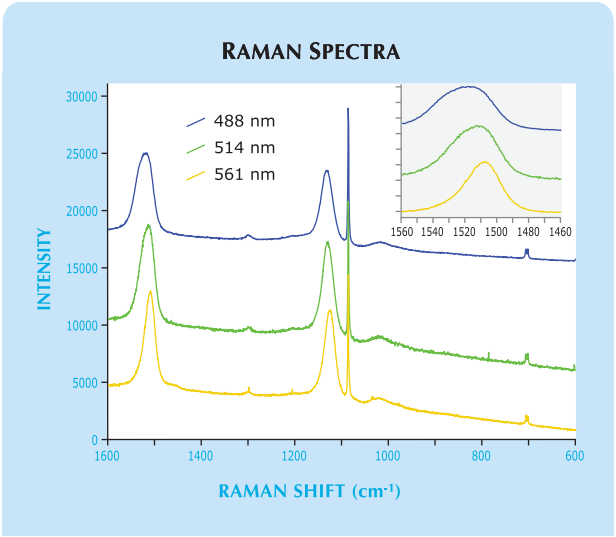

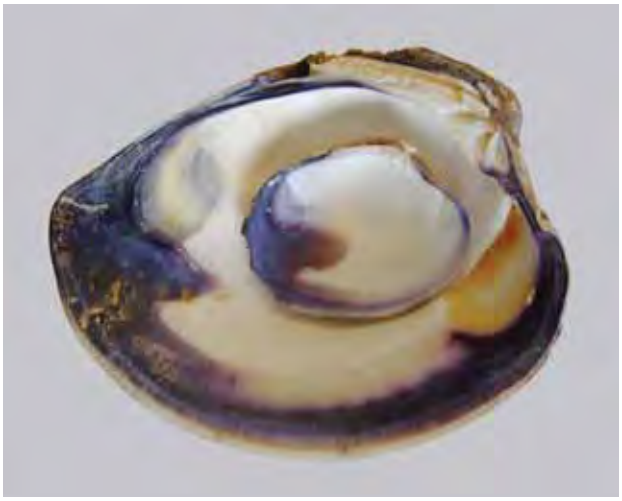

Figure 15. Though V. aff. decussata *(inner shell, 4.5 cm) is found on the western coast of France and* M. mercenaria *(9.5 cm, courtesy of Antoinette Matlins, South Woodstock, Vermont) is found on the North American Atlantic coast, the two exhibit similar coloration. Photo by S. Karampelas.*

observed in freshwater cultured pearls (S. Karampelas et al., "Identification of pigments in freshwater cultured pearls with Raman scattering," Fall 2006 *Gems & Gemology*, pp. 99–100).

M. mercenaria can reach 12 cm in diameter, while *V. aff. decussata* mollusks from the west coast of France do not exceed 7.5 cm. Thus, the latter mollusks produce smaller pearls (rarely up to 6 mm) compared to those from *M. mercenaria* (rarely up to 12 mm). It should be noted that "gem-quality" natural pearls from *V. aff. decussata* have been documented only once, whereas there have been numerous reports of gem-quality quahog pearls.

Stefanos Karampelas (s.karampelas@gubelingemlab.ch)
Department of Geology, University of Thessaloniki, Greece;

Institut des Matériaux Jean Rouxel (IMN)
University of Nantes, France

Emmanuel Fritsch

Franck Notari

SYNTHETICS AND SIMULANTS

Synthetic citrine with abundant nail-head spicules. A necklace of transparent yellow faceted beads (figure 17) was sent to Gemlab for identification. Specular reflectance Fourier-transform infrared (FTIR) spectroscopy identified the material as quartz. FTIR spectra recorded in transmission mode were not definitive, but nevertheless were characteristic of synthetic citrine. The spectra contained an unusually intense water absorption centered at ~3200 cm^{-1} (too strong to be resolved) and only a single sharp peak at 3580 cm^{-1}. In general, natural citrine has a much lower water content and shows more complex FTIR spectra.

Figure 17. This necklace, submitted to the Gemlab Laboratory for identification, contained 49 faceted beads (~20 mm diameter) of what proved to be synthetic citrine. Photo by T. Hainschwang.

Microscopic examination revealed a most unusual inclusion scene: All of the beads were full of hollow growth channels (figure 18, left) and nail-head spicules (wedge-shaped, liquid-filled growth channels terminated by an inclusion on one end; figure 18, right). Nail-head spicules are characteristic inclusions in both synthetic beryl and synthetic quartz, though similar-looking inclusions have been described in some natural stones (G. Choudhary and C. Golecha, "A study of nail-head spicule inclusions in natural gemstones," Fall 2007 *Gems & Gemology*, pp. 228–235). Thus, isolated inclusions of this type do not necessarily offer proof of synthetic origin.

Nevertheless, the appearance of the nail-head spicules in these beads was typical for synthetic material, especially since the "heads" of the spicules contained "breadcrumb" inclusions (e.g., figure 19), the most characteristic and common inclusion in synthetic quartz. However, this contributor has never seen such a large number of these inclusions in any type of synthetic material. All of them exhibited the typical wedge shape, and in most of them the liquid contained a gas bubble.

The inclusions, hollow cavities, and nail-head spicules were oriented parallel to the c-axis. In determining the optic axis direction, it was evident that none of the material was twinned—unlike most natural citrine, which is created by heat-treating natural amethyst that commonly contains Brazil-law twinning. The large, hollow cavities likely represent oversized nail-head spicules that were either exposed by the polishing process or reached the surface during the growth process. In some of these very large cavities, the breadcrumb inclusion was found at the narrow end of the channel (figure 20, left); in the others, it was absent (figure 20, right). These features, like the smaller nail-head spicules, can probably be attributed to rapid growth conditions.

The necklace, which had been sold to the client as natural quartz, was therefore identified as synthetic citrine. Despite this deception, the piece was a fantastic source of photomicrographs of nail-head spicules, which normally do not occur in such heavy concentrations.

Thomas Hainschwang
(thomas.hainschwang@gemlab.net)
Gemlab Laboratory for Gemstone Analysis and Reports
Balzers, Liechtenstein

Radiocarbon dating of "Neptunian" beads from Asia proves modern origin. During the inaugural Macau Jewellery & Watch Fair in January 2008, this contributor purchased four baroque-shaped drilled beads of an unknown material that were sold as Neptunian beads. The brownish orange samples had white striae, and the brownish orange portions showed an appealing sheen (figure 21). When asked about their origin, the seller reported that the material was from fossilized conch shell found at an altitude of 5,000 m in the Himalaya Mountains. A brochure provided with the samples added that the beads had several medicinal uses.

In the laboratory, we found that the specific gravity of the beads was 2.78. Close examination showed that they had two folded layers, which is common for conch shell (figure 22). Raman spectroscopy identified the material (both the orange and white portions) as aragonite. EDXRF analysis

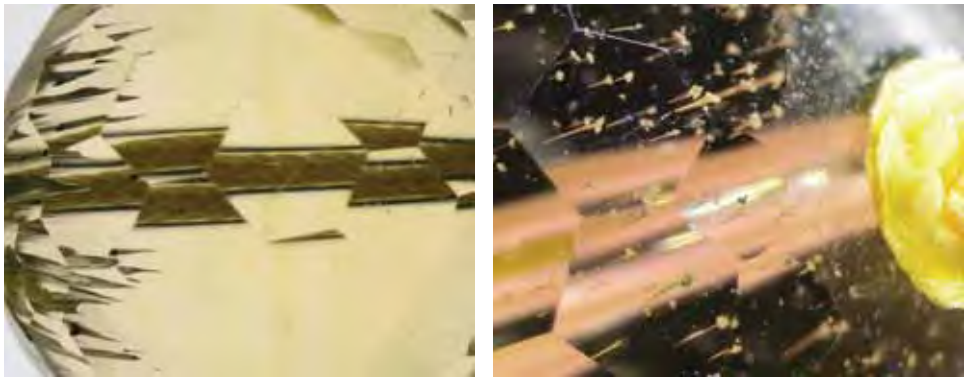

Figure 18. The inclusion scene in the beads consisted of hollow growth tubes (left) and nail-head spicules (right), which are often seen in synthetic quartz and beryl. Photomicrographs by T. Hainschwang; field of view is 18 mm (left) and 10.5 mm (right).

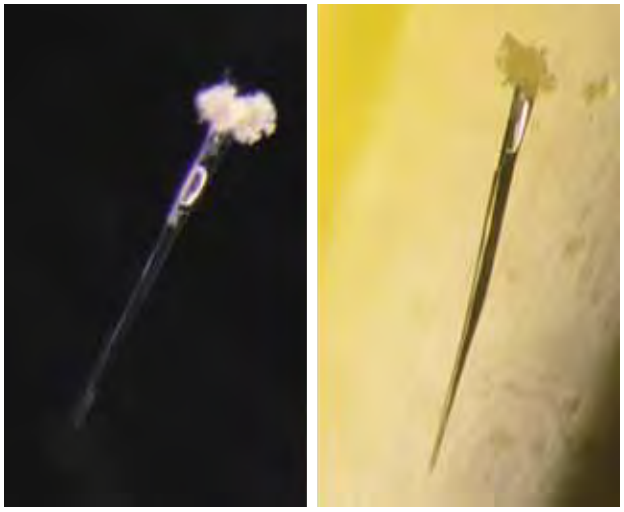

Figure 19. The nail-head spicules in the synthetic quartz beads, such as those shown here, consist of liquid-filled cavities that may contain a gas bubble and be terminated by a "breadcrumb" inclusion. Photomicrographs by T. Hainschwang; field of view is ~1 mm high for both.

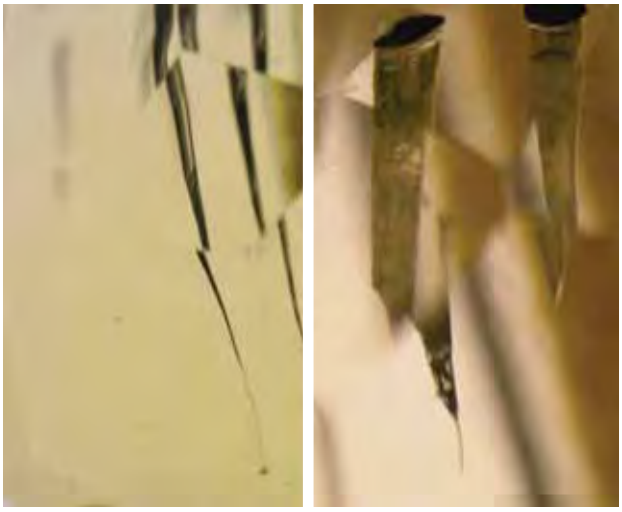

Figure 20. Some of the surface-reaching hollow cavities in the synthetic citrine beads (e.g., as shown in figure 18) showed a breadcrumb inclusion at their narrow end (left) while others did not (right). Photomicrograph by T. Hainschwang; field of view is 5.4 mm high (left) and 4.1 mm high (right).

showed that Ca was the only major element, with traces of Sr present, as expected for aragonite from conch shell.

However, the material did not have the appearance of a fossil, so the author decided to apply a method rarely used in gemology: age determination by radioisotope. The Swiss Federal Institute of Technology (SFIT) in Zürich performed ^{14}C isotope measurement to calculate the age (radiocarbon dating can determine ages up to 30,000 years). To make the determination, the laboratory took 200 mg of powder from the drill hole of one of the beads.

A spectrum relating time with atmospheric radiocarbon content and the sample's data is shown in figure 23. Because above-ground nuclear weapons testing in the 1950s substantially raised the concentration of ^{14}C in the atmosphere (and consequently in all living organisms), the testing produced two possible results (see P. J. Reimer et al., "Discussion: Reporting and calibration of post-bomb ^{14}C data," *Radiocarbon*, Vol. 46, No. 3, 2004, pp. 1299–1304).

Figure 21. These baroque-shaped beads, marketed as fossilized Neptunian beads, proved to be recent shell material. The largest bead is ~17 mm long. Photo by H. A. Hänni, © SSEF.

The $^{12}C/^{14}C$ ratio of the sample intersected with the atmospheric ratio at 1957 and 1997. Clearly, the beads are far younger than the 35 million years claimed in the brochure.

Henry A. Hänni

Purplish blue synthetic quartz. Synthetic quartz has long been available in a wide range of colors, such as yellow, purple-violet, green, pink, colorless, parti-colored, and even blue. Recently, the Gem Testing Laboratory of Jaipur, India, had an opportunity to study a new and unusual "cobalt" blue synthetic quartz.

Figure 22. The beads consist of alternating layers of nacreous orange and non-nacreous white aragonite. Photo by H. A. Hänni, © SSEF; image width 16 mm.

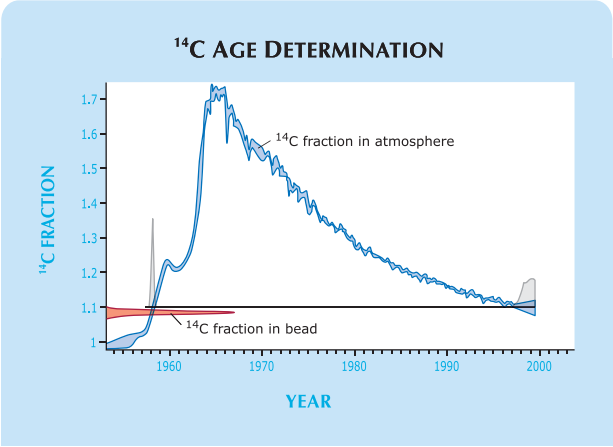

Figure 23. The ^{14}C distribution and the two maxima in gray indicate that the aragonite from a Neptunian bead originated in either 1957 or 1997. The Y-axis shows the $^{12}C/^{14}C$ ratio measured in the bead normalized to the $^{12}C/^{14}C$ ratio of the standard. Graph courtesy of G. Bonani and I. Hajdas, SFIT; © SSEF.

Figure 24. This bright "cobalt" blue specimen (73.08 g) proved to be synthetic quartz. Note the "cobbled" surface with circular growth patterns. Photo by G. Choudhary.

A purplish blue specimen weighing 73.08 g was submitted for identification. At first glance, the specimen appeared to be a cobalt glass because of its color (figure 24) and apparently frosted surface. However, we observed tiny circular growth features that were very similar to the "cobbled" surface seen in rough slabs of synthetic quartz. When the specimen was viewed from the side, a colorless zone with the appearance of a seed plate was evident, which led us to believe that the material was actually synthetic quartz.

The specimen displayed a clear anisotropic reaction when rotated in the polariscope, confirming that it was not glass. A bull's-eye optic figure—as expected for quartz—could not be resolved, due to the rough surfaces. With the desk-model spectroscope, however, we observed three strong bands in the green, yellow, and orange regions; this absorption pattern is typical of cobalt. The sample had a strong red reaction to the Chelsea filter, and was inert to long- and short-wave UV radiation.

Examination with magnification confirmed the presence of a seed plate. Also seen was color zoning parallel to the seed plate, as well as nail-head spicules along its length (figure 25). An interesting aspect was the location/orientation of the spicules. In general, nail-head spicules are oriented in one direction pointing away from the seed

Figure 25. When the sample in figure 24 was viewed from the side, a seed plate was visible (white arrows) along with nailhead spicules that for the most part were restricted to the seed plate (red arrows). Also note the blue color zoning parallel to the seed; the diagonal features are surface-related optical effects. Photomicrograph by G. Choudhary; magnified 30×.

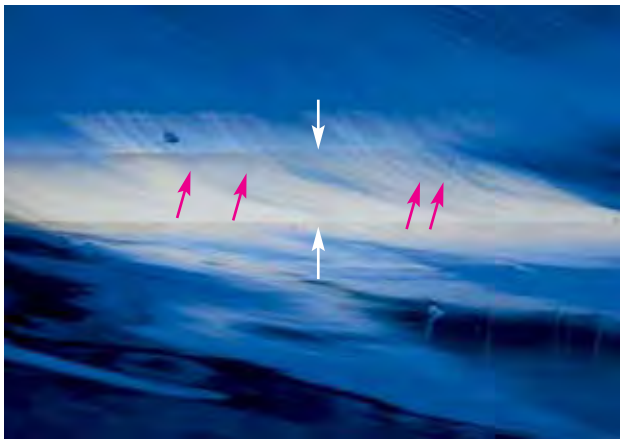

Figure 26. At higher magnification, the spicules in the seed plate appeared to be oriented in different directions. The central colorless seed plate is separated from the synthetic quartz overgrowth by sharp planes on either side (see arrows). Photomicrograph by G. Choudhary; magnified 65×.

Figure 27. This 45.78 ct cabochon resembling chrysocolla proved to be dyed chalcedony. Photo by N. Ahmed, © Dubai Gemstone Laboratory.

Figure 28. Microscopic examination of the dyed chalcedony shows a greenish blue dye concentrated in fractures and cavities. Photomicrograph by N. Ahmed, © Dubai Gemstone Laboratory; magnified 20×.

plate, on both sides of the synthetic overgrowth. In this case, however, most of the spicules appeared to be in the seed plate rather than in the overgrowth material. At some viewing angles, the spicules appeared to be oriented in different directions (figure 26).

While the influx of interesting colors of synthetic quartz has given jewelers more options, proper disclosure remains essential.

Gagan Choudhary

TREATMENTS

Dyed chalcedony resembling chrysocolla. Historically, chalcedony has been dyed in a wide variety of colors, often to simulate various other gem materials. Recently, the Dubai Gemstone Laboratory received for identification a 45.78 ct greenish blue cabochon with areas of orangy brown (figure 27). At first glance, the semitranslucent-to-opaque stone resembled chrysocolla. An SG of 2.29 (determined hydrostatically) and a vague RI reading around 1.5 supported this initial impression (R. Webster, *Gems*, 5th ed., revised by P. G. Read, Butterworth-Heinemann, Oxford, UK, 1994, pp. 326–327). The stone did not exhibit strong reactions to long- or short-wave UV radiation, only a weak, patchy bluish green fluorescence to long-wave UV. The stone's Chelsea filter reaction was pinkish red.

Examination with magnification (up to 68×) did not reveal the minute chrysocolla inclusions present in chrysocolla chalcedony, although such inclusions are typically too small to see with a gemological microscope. However, microscopic examination did reveal that the surface-reaching fractures and cavities had concentrations of a greenish blue dye (figure 28), which could be removed with acetone.

Colorless-to-milky chalcedony can easily be dyed with inorganic cobalt or copper salts to simulate chrysocolla (see A. Shen et al., "Identification of dyed chrysocolla chalcedony," Fall 2006 *Gems & Gemology*, p. 140). However, because of the stone's opacity, we did not obtain the characteristic absorption lines of chalcedony dyed with cobalt, and we were unable to perform UV-Vis-NIR spectroscopy to compare our data with those of Shen et al.

Nevertheless, all of these properties pointed to dyed chrysocolla or dyed chalcedony. Raman analysis is unable to differentiate between chrysocolla and chalcedony. However, EDXRF spectroscopy showed a major amount of Si and only traces of Fe, identifying the material as chalcedony. By contrast, chrysocolla is a hydrous copper silicate [$(Cu,Al)_2H_2Si_2O_5(OH)_4 \cdot nH_2O$], and no Cu was detected in the sample. Therefore, the client was informed that the cabochon consisted of dyed chalcedony.

Nazar Ahmed (nanezar@dm.gov.ae)
Dubai Gemstone Laboratory
Dubai, United Arab Emirates

ANNOUNCEMENTS

Starting with this issue, the conference and exhibit calendars will only appear online at www.gia.edu/gemsandgemology. Please refer to this online resource for regular updates to these calendars.